Calf-Thymus Topoisomerase I Equilibrates Metastable Secondary Structure Subsequent to Relaxation of Superhelical Stress

ARTICLE *in* BIOCHEMISTRY · FEBRUARY 2010

Impact Factor: 3.02 · DOI: 10.1021/bi9017126 · Source: PubMed

3 AUTHORS, INCLUDING:

Jeffrey Delrow
Fred Hutchinson Cancer Research Center
84 PUBLICATIONS **5,071** CITATIONS
SEE PROFILE

J. Michael Schurr
University of Washington Seattle
178 PUBLICATIONS **4,100** CITATIONS
SEE PROFILE

BIOCHEMISTRY
including biophysical chemistry & molecular biology
Article

Biochemistry **2010,** *49,* 3367–3380 3367
DOI: 10.1021/bi9017126

Calf-Thymus Topoisomerase I Equilibrates Metastable Secondary Structure Subsequent to Relaxation of Superhelical Stress

Greg P. Brewood, Jeffrey J. Delrow, and J. Michael Schurr*

University of Washington, Department of Chemistry, Box 351700, Seattle, Washington 98195-1700

Received October 3, 2009; Revised Manuscript Received February 9, 2010

ABSTRACT: After relaxation of superhelical stress by various methods not involving topoisomerases, a long-lived metastable secondary structure with an anomalously low torsion elastic constant commonly prevails. The aim here is to ascertain whether such metastable secondary structure also results from the action of calf-thymus topoisomerase I (CT Topo I) on a native supercoiled DNA and, if so, whether the enzyme catalyzes its subsequent equilibration. The action of CT Topo I on supercoiled p30δ DNA was examined over a range of times from 10 min to 6 h. We verify that the enzyme operates in an almost completely processive manner, and at each time point determine the twist energy parameter, E_T, that governs the supercoiling free energy. E_T is initially low, 533 ± 60, and remains essentially constant up to at least 360 min, when no further CT Topo I is added. The activity of the rather dilute enzyme dies within ~60 min. During the 60 min after a second addition of fresh enzyme at either 60 or 120 min, E_T rises up to a plateau at ~1100, which lies within the consensus equilibrium range, 1000 ± 100. Over that same time period, the average peak spacing between the gel bands (corresponding to individual topoisomers) decreases somewhat with increasing time of exposure to active CT Topo I. After a third addition of fresh CT Topo I at 240 min, there is no further change in either E_T or the average gel spacing. These and other observations indicate that active CT Topo I catalyzes the equilibration of a metastable secondary structure with abnormally low torsion and bending elastic constants that prevails after the initial release of superhelical stress. An observed temporal lag of this structural equilibration behind the relaxation of native superhelical DNAs suggests that it may require cleavage and religation events at multiple sites on the DNA. A novel analysis of the unwinding kinetics using literature data accounts for the almost complete processivity of the enzyme. The action of CT Topo I was also examined in the presence of 20 and 40 w/v% ethylene glycol (EG), which shift a secondary structure equilibrium toward an alternative state with altered torsion and bending elastic constants. The present results suggest that the usual metastable state coexists with the EG-induced state, and is equilibrated more rapidly than in the absence of EG.

Long-lived metastable secondary structure with an anomalously low torsion elastic constant commonly prevails in large circular DNAs for up to 2 weeks or more after relaxation of native superhelical stress by any of three methods: (i) linearization (*1*−*3*), (ii) binding sufficient intercalating dye molecules (*3*−*7*), or (iii) binding sufficient *E. coli* single-strand binding protein (SSB) (*3*, *8*). Full equilibration to attain the normal torsion elastic constant may require up to 10 weeks after relaxation of the superhelical stress. Such metastable secondary structure is likely related to variations in equilibrium structure with superhelix density (σ) that were observed over the intermediate range, $-0.035 \leq \sigma \leq -0.010$, for pUC8 dimer (*2*) and pBR322 (*7*) in a low salt (10 mM NaCl) buffer. Such variations in secondary structure were manifested by *minima* in: (i) the torsion elastic constant (α) measured by time-resolved fluorescence polarization anisotropy (FPA), (ii) the circular dichroism at 250 nm (CD_{250}), and (iii) the dynamic light scattering diffusion coefficient (D_{plat}) at large scattering vector ($K = 4.5 \times 10^5$ cm^{-1}), which declines with decreasing torsion elastic constant. In either 10 or 100 mM NaCl, kinetic trapping of at least part of the sequence in a metastable state with a low torsion elastic constant commonly occurs, when the superhelix density traverses from the native value ($\sigma \simeq -0.05$) toward zero through this intermediate region. Cumulative evidence from our lab suggests that the long-lived metastable secondary structure subsequent to linearization of native supercoiled DNAs is more likely to be observed in 10 mM NaCl than in 100 mM NaCl, but may still occur in the latter. Although various procedures, including exposure of DNA samples to elevated temperatures or to high salt concentration for different periods of time, were performed in an attempt to accelerate the equilibration process, none proved satisfactory for reasons indicated below.

Slow changes in α, CD at 270 nm (CD_{270}), and D_{plat} were commonly observed over several days or more in the responses of certain linear DNAs to various changes in conditions, including cyclic variations of either salt concentration or temperature, and the binding of less than 1 ethidium per 300 bp in 4.5 M NaCl (*3*, *9*). The evident metastability and hysteresis in such cases were ascribed to slowly relaxing, cooperative, allosteric transitions among conformational substates within the B-family, as described elsewhere (*10*). Although the structures of the various conformational substates are not known in any detail, certain observations suggest that their intrinsic twists are similar, and that their intrinsic curvatures differ significantly in at least some cases. In particular, the dynamic torsion elastic constant measured for unstrained or very weakly strained DNAs by the FPA method is practically identical to the equilibrium (static) value inferred from equilibrium

*To whom correspondence should be addressed. E-mail: schurr@chem.washington.edu. Telephone: 206-543-6681. Fax: 206-685-8665.

Published on Web 02/23/2010

topoisomer distributions (*11*). However, the dynamic bending elastic constant, assessed by either a transient polarization grating (TPG) method (*12*) or EPR-spin label methods, (*13*−*15*) is 3 to 4 times greater than the equilibrium value obtained via cyclization kinetics measurements on small circular DNAs (*16*). The implied softening of the bending elastic constant (κ_β), but not the torsion elastic constant on a sufficiently long time-scale ($t > 10^{-5}$ s) is attributed to a kinetically slow conversion of some of the sequence from an intrinsically less curved to an intrinsically more curved conformation with practically the same intrinsic twist (*12*). The elastic constants for torsion and bending, α and κ_β, apply to the effective springs between base-pairs, and are related to the corresponding rigidities by, $C = \alpha h$ and $A = \kappa_\beta h$, respectively, where h is the rise per bp (*1*−*12*).

The prevalence of long-lived metastable secondary structure in many DNAs subsequent to relaxation of superhelical stress has been a significant (and doubtless often unrecognized) obstacle to reliable and reproducible measurements of various structure-sensitive properties. Consider, for example, the twist energy parameter (E_T), which governs the supercoiling free energy. E_T is proportional to the Hooke's law torque constant for supercoiling and increases monotonically with the elastic constants, α and κ_β. Measurements of E_T by intercalator binding methods commonly yielded anomalously low values, $E_T \leq 500$ (c.f. Table II of ref *4*) (*4*, *7*, *17*−*19*), which are about half or less of the generally accepted values, $900 \leq E_T \leq 1100$, which were obtained by the topoisomer distribution method (c.f. Table I of ref *4*) (*20*−*24*), and also via the ethidium binding method for a sufficiently equilibrated sample of p30δ DNA in a standard 100 mM NaCl buffer (*24*). Numerous Monte Carlo simulations and reversible work calculations for model DNAs with the consensus persistence length, $P = 500$ Å, a torsion elastic constant in the range, $5.0 \times 10^{-12} \leq \alpha \leq 6.5 \times 10^{-12}$ erg (obtained via FPA measurements on equilibrated unstrained DNAs), and appropriate interduplex repulsive potentials yielded E_T-values in the consensus range, $900 \leq E_T \leq 1100$ (*11*, *25*−*27*). Substantially (≤0.5-fold) lower torsion and/or bending elastic constants would be required to yield, $E_T \lesssim 500$. Such low elastic constants are presumably associated with long-lived metastable secondary structure.

Some DNAs, such as p30δ, are much less prone to exhibit long-lived metastable secondary structure (following changes in superhelical stress) than are other DNAs, such as pBR322 (*7*) and pUC8 (*2*), despite their identical superhelix densities, preparation methods, and sample conditions (*24*). For that reason our lab has worked primarily on p30δ since the early 1990s. Nevertheless, even for p30δ DNA, modest but statistically significant variations in properties among five identically prepared native supercoiled samples in 100 mM NaCl suggest that at least parts of their sequences may also undergo ultra-slow equilibration subsequent to whatever change in superhelical stress occurs during the isolation and purification process (*28*). Moreover, measurements of CD_{270} for p30δ DNA in a low salt (10 mM NaCl) buffer before and after linearization yielded the temporal trajectory indicated in Table 1. This trajectory is qualitatively similar to those observed for the torsion elastic constants of pBR322, pUC8, and the replicative form of M13mp7 under similar conditions (shown in Figure 4 of ref *2*). Specifically, CD_{270} declines to a minimum between 1 and 2 weeks, after which it evolves upward toward its eventual equilibrium value. This implies that extensive metastable secondary structure extending over a substantial fraction of the sequence persists for over two weeks after linearization of this sample.

There arises the question of why E_T measurements obtained via the topoisomer distribution method have so far not exhibited the low values often (but not always) obtained via intercalator binding methods. An obvious possibility is that the topoisomerase I, which was employed to relax the native superhelical stress and create the "equilibrium" distribution of topoisomers (with an E_T-value appropriate for the prevailing secondary structure), also catalyzes the equilibration of any metastable secondary structure that forms immediately upon release of superhelical stress. If topoisomerase I should have the ability to equilibrate such metastable secondary structure, as will be shown, it could be used to improve the reliability and reproducibility of experimental measurements of structure-sensitive properties of various DNAs, especially those that have recently undergone significant changes in superhelical stress. It is also conceivable that metastable secondary structures formed in response to varying conditions in vivo, such as alterations of superhelical stress during the cell cycle, could interfere with normal gene activation and/or repression. In that case, such a second function of topoisomerase I to equilibrate metastable secondary structure might be biologically significant. Hence it is important to learn whether a typical topoisomerase I functions in such a manner.

With increasing concentration of ethylene glycol (EG), p30δ DNA undergoes a transition to an alternative secondary structure with a ∼0.2% smaller intrinsic twist, a ∼0.91-fold smaller value of E_T, a 2.0- to 2.1-fold greater torsion elastic constant, and a ∼0.70-fold smaller bending elastic constant (*29*−*32*). The midpoint of the transition occurs near 20 w/v% EG. This raises the question of whether metastable secondary structure also persists when a supercoiled DNA is relaxed by CT Topo I in 20 w/v% EG, and, if so, whether it is equilibrated more rapidly or slowly than in the absence of EG.

It was previously shown that human topoisomerase I always gave rise to an approximately bell-shaped envelope of the relaxed topoisomer populations in the gel with no visible intermediate species (*33*, *34*). From this it was concluded that the enzyme operates in a largely processive manner, meaning that a substantial fraction of the original mean linking difference is shed in the first encounter between the enzyme and DNA. This conclusion was supported by a study of *Vaccinia* topoisomerase I acting on a supercoiled DNA under conditions where the DNA was saturated with enzyme (*35*). By fitting a kinetic model to the observed temporal evolution of the native supercoiled DNA, relaxed "products", and intermediate topoisomers, values were obtained for the cleavage and religation rate constants and the rate of rotation, which was assumed to be constant. From the results it was estimated that about 5 supercoils were shed per cleavage and religation event. This should be regarded as an estimated lower bound for the extent of processivity, which in principle could be much greater, depending upon the average number of cleavage and religation events that occur before the enzyme dissociates from the DNA. This latter number could not be obtained under the prevailing conditions, and no estimate was made of the full extent of processivity. An additional problem is that the kinetic model of Stivers et al. (*35*) takes no account of the expected proportionality between the rotation (unwinding) rate and the torque driving the unwinding, which in a circular DNA is proportional to the declining superhelix density. In this regard, the model is somewhat unrealistic.

Variation of the mean rate of unwinding with applied torque was demonstrated by Koster et al. (*36*), who examined the unwinding during individual cleavage and religation events in a

Table 1: Temporal Trajectory of CD_{270} for a Sample of p30δ Subsequent to Linearization in a Low Salt Buffer[a]

sample	CD_{270} (mdeg)
native sc[b]	1.71
linearized +3 days	1.20
linearized +11 days	0.70
linearized +17 days	1.11
linearized (equilibrium)	1.65

[a]Buffer contains 10 mM NaCl, 10 mM Tris·HCl, 1 mM EDTA. [b]Superhelix density is, $\sigma \simeq -0.05$.

single twisted linear DNA with torsionally clamped ends that was held at a constant (but adjustable) tension in the presence of different type Ib topoisomerases. They also demonstrated that both *Vaccinia* and human topoisomerases exerted significant friction on the unwinding motion. In the case of *Vaccinia* topoisomerase I, it was found that about 15 supercoils were shed per cleavage and religation event at the prevailing torque. However, no attempt was made to infer from these findings the quantitative extent of processivity of either *Vaccinia* or human topoisomerase I, when acting upon a supercoiled circular DNA, where the torque is both different and decreasing with time.

Neither of the studies discussed above suffices to show that the processivity is complete, in the sense that practically all of the original linking difference of the circular DNA is shed before the enzyme dissociates, so an equilibrium, or very nearly equilibrium, distribution of topoisomers is attained in the very first encounter between the enzyme and DNA. In order to demonstrate the latter, one must verify quantitatively that the relative populations of relaxed topoisomers at all times exhibit the predicted equilibrium Gaussian shape when plotted vs excess linking number (relative to that of the most populous topoisomer), and also that the center of the distribution does not shift significantly with increasing time of exposure to active enzyme. Such tests were not undertaken in previous studies.

Until now, there has appeared no quantitative analysis of any kinetic model for relaxation of a supercoiled circular DNA by a eukaryotic topoisomerase I that takes into account both the previously unknown friction coefficient and the declining torque associated with the unwinding motion, from which the extent of processivity can be estimated.

The principal goal of this study is to examine the "relaxed" topoisomer distributions formed by the action of calf-thymus topoisomerase I (CT Topo I) at different times after adding the enzyme to native supercoiled p30δ. We begin with the earliest time, 10 min, at which relaxed topoisomers appear in sufficient amounts to permit a quantitative, albeit somewhat noisy, assessment of their relative populations. Particular attention is paid to the distribution of relaxed topoisomers, the value of E_T implied by that distribution, and the temporal trajectory of E_T with time. At each sample time the linking difference of the most abundant topoisomer is assessed, the average peak spacing between topoisomer bands in the gel is reckoned, and finally the temporal trajectories of both quantities are recorded. We also search for partially relaxed topoisomers with gel mobilities intermediate between those of the apparently fully relaxed topoisomers and those of the still unaltered native supercoiled DNAs. From such information, we verify that CT Topo I operates not merely in a largely processive manner, as concluded previously, but in an almost completely processive manner.

A novel analysis of the kinetics of unwinding of a supercoiled circular DNA is undertaken below. By using certain kinetic and equilibrium constants from the literature (*35*, *37*) along with an appropriate and declining value of the torque, and a value of the friction coefficient extracted from the equilibrium and dynamic data of Koster et al. (*36*) (J. M. Schurr and B. S. Fujimoto, Ms. in preparation), a quantitative estimate of the extent of processivity can be obtained. The results support the observed almost complete processivity of the enzyme.

The measured E_T-values are combined with measured or estimated torsion elastic constants to estimate the effective bending elastic constants and persistence lengths of both the metastable and equilibrium states of relaxed supercoiled DNAs.

The effect of ethylene glycol on the relaxation of p30δ DNA by CT Topo I is also briefly investigated in order to ascertain whether the existence and rate of equilibration of the metastable state are affected by the presence of EG.

MATERIALS AND METHODS

The sequence of p30δ (4932 bp) is identical to that of pBR322 (4363 bp) over ~4000 bp. It was constructed by inserting 842 bp containing the Bg*l*II to *Sal*I fragment of *S. cerevesiae* between the *Bam*HI and *Sal*I sites of pBR322 (*38*). Its sequence was unambiguously determined by recent direct sequencing (*31*). Isolation and purification of p30δ were performed as described previously (*32*). The plasmid was dialyzed into storage buffer containing 50 mM KCl, 50 mM Tris, 0.1 mM EDTA, pH 7.5, and kept at 4 °C. The A_{280}/A_{260} ratio was ~1.9 and an analysis of band intensities following gel electrophoresis indicated a supercoiled:nicked ratio greater than 4:1.

Topoisomerization of native supercoiled p30δ was carried out at 37 °C by one, two, or three additions of CT Topo I from Invitrogen to obtain a reaction mixture of final composition: 0.1, 0.2, or 0.3 units of CT Topo I/μL, 50 mM KCl, 50 mM Tris, 0.1 mM EDTA, 10 mM $MgCl_2$, 30 μg/mL bovine serum albumin, 0.5 mM dithiothreitol, 2.5 w/v% glycerol, and 25 μg/mL DNA, pH 7.5. The molar concentration ($[E_0]$) of initially active enzyme can be estimated approximately from the definition of 1 unit, which is the amount required to relax 0.5 μg of *φX* RF DNA (3.57×10^6 Da), equivalent to 1.4×10^{-13} mol DNA, in 30 min, presumably under enzyme-saturated conditions. Under such conditions the rate is, $R = k_{cat}[E_0]$ mol L^{-1} s^{-1}, where k_{cat} is approximately equal to the rate-limiting product dissociation rate constant, which was reported to be about 0.06 s^{-1} for human Topo I acting on SV40 DNA under conditions similar to those used here (*37*). Assuming that such a value applies also to CT Topo I in the present study, we estimate that, $[E_0] = R/k_{cat} = 1.4 \times 10^{-13}/((1800)(0.06)) = 1.3 \times 10^{-6}$ nM for 1 unit/L. The reaction mixtures in this study contain 0.1−0.3 units/μL, which corresponds to 0.13−39 nM. The 25 μg/mL concentration of p30δ (3.28×10^6 Da) corresponds to 7.6 nM, so the substrate is estimated to be in ~19−58-fold excess in our experiments. Aliquots were withdrawn from the reaction mixture at either 10 or 20 min intervals, and their reactions were halted immediately by extracting the enzyme once with a mixture of phenol, 0.1 w/v% 8-hydroxyquinoline, 48 v/v% chloroform, and 2 v/v% isoamyl alcohol, as done previously (*30*−*32*). The phenol/8-hydroxyquinoline was pre-equilibrated with buffer containing 0.2 mM NaCl and 0.1 mM Tris at pH 8.0.

Topoisomerization products were subjected to electrophoresis for 48 h in 0.8 w/v% agarose gels, wherein sufficient (0.08 μg/mL)

chloroquine was incorporated to shift the linking differences of all visible relaxed topoisomers into the zero to slightly positive range, as described previously (*24*, *30*−*32*). Treatment of the gel to remove chloroquine and to stain the DNA with ethidium under conditions, where the amount bound is proportional to the relative concentration of any visible topoisomer, was carried out as described previously (*24*, *30*−*32*). The fluorescence in the gel was imaged and quantitated with a Fluoroimager SI gel scanner and the integrated intensity of each peak was reckoned using commercial software (ImageQuant 5.1), as described previously (*30*−*32*).

The most abundant topoisomer (i.e., peak of greatest integrated intensity) has the integral linking number (l_{mp}) nearest to the intrinsic twist (l_0) under reaction conditions, denoted by $l_{mp} = \mathrm{NINT}(l_0)$, and all of the topoisomers are simply indexed by their excess linking number (l_{ex}) relative to l_{mp} as, $l_{ex} = \ldots -3, -2, -1, 0, +1, +2, +3 \ldots$. The measured ratio of the peak intensities, $I_{l_{ex}}/I_0$, is assumed to equal the corresponding ratio of topoisomer concentrations, $c_{l_{ex}}/c_0$, under reaction conditions. The various ratios for the readily observable peaks are fitted by the following expression for an equilibrium distribution (*30*−*32*),

$$c_{l_{ex}}/c_0 = \exp\left[-(E_T/N)\left((l_{ex}+\Delta l_0)^2 - \Delta l_0^2\right)\right] \qquad (1)$$

with E_T and the linking difference of the most abundant topoisomer under reaction conditions, $\Delta l_0 = l_{mp} - l_0$, as adjustable parameters. The procedure was described previously (*24*, *30*, *32*).

The activity of CT Topo I to relax superhelical turns (i.e., decrease the native supercoiled peak), did not remain constant after Topo I addition to the DNA sample, but instead died within ~60 min, presumably due to contaminating proteases in the commercial Topo I preparation, and/or a finite probability that enzyme/DNA complexes fail to religate after a cleavage event, and/or slow irreversible thermal denaturation of the enzyme. In any event, this necessitated multiple additions of fresh enzyme to the reaction mixture at various times after initiation of the reaction in order to drive the topoisomerization to completion.

Because only a single reaction mixture was run at any given time, the present data for the time course of E_T are considerably noisier than values obtained for completed reactions in our previous studies (*30*, *32*), where at least 12 parallel reactions were run to completion for each set of conditions. Nevertheless, the data provide a reasonable estimation of the temporal trajectory of E_T.

We endeavored to measure any changes in electrophoretic mobility with increasing time of exposure to active enzyme. Because the maximum variation in migration distance among the samples was smaller than variations due to intrinsic differences between gels, comparisons were restricted to different lanes in the same gel. When the mobilities change from one reaction time to the next, such changes are typically greater for topoisomers with larger excess linking numbers. Satisfactory precision was obtained by taking the difference in migration distance between topoisomers with high, $l_{ex} = +3$, and low, $l_{ex} = -3$, excess linking numbers in the same lane. This is equivalent to using the $l_{ex} = -3$ topoisomer in place of the nicked circle as the internal standard in each lane, which offers potentially greater accuracy. The $l_{ex} = -3$ topoisomer is typically close to, but not overlapped by, the nicked circle band, so its linking difference in the gel is ~ +1, and that of the $l_{ex} = +3$ topoisomer is ~+7. The $l_{ex} = -3$ and +3 topoisomers are more likely to contain similar amounts of metastable secondary structure, and their mobilities

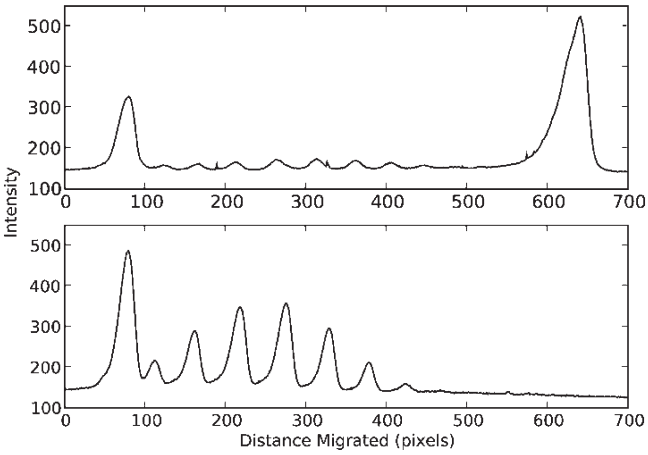

FIGURE 1: Intensity of ethidium fluorescence vs distance migrated (in pixels). Data are obtained from scans of the fluorescence images of the two corresponding gel lanes. (Top) A sample of p30δ that received a single addition of 0.1 unit of CT Topo I/μL at $t = 0$ min and was assayed at $t = 40$ min. (Bottom) A sample of p30δ that received three additions of 0.1 unit of CT Topo I/μL at, respectively, $t = 0$, 120, and 240 min, and was assayed at 360 min. Reaction conditions are as described under Materials and Methods. The large peak on the far left comprises nicked circles, and that on the far right comprises native supercoiled DNAs. The lower peaks between those two peaks are relaxed topoisomers.

are more likely to be similarly affected by extraneous buffer components or non-extracted enzyme than would be the case for nicked circles and $l_{ex} = +3$ topoisomers. When the mobility difference between the $l_{ex} = -3$ and $l_{ex} = +3$ topoisomers is divided by 6, it becomes just the average spacing between peaks of the 7 most populous topoisomer bands, and that is the quantity reported here.

Topoisomerization reactions and gel electrophoretic analyses of the reaction products at 10 min intervals were also carried out in the presence of 20 and 40 w/v% ethylene glycol. In such cases the DNA sample was equilibrated with either 20 or 40 w/v% ethylene glycol before the CT Topo I was added.

RESULTS AND DISCUSSION

Qualitative Aspects of the Mechanism of Topoisomerization by CT Topo I in Aqueous Solution. All of our observations are consistent with a mechanism, wherein bound CT Topo I operates in an almost completely processive manner to relax practically all of the superhelical turns of the DNA to which it is attached, before dissociating therefrom. This conclusion is inferred from the following observations pertaining to topoisomerization.

(1) Fluorescence scans of gel lanes containing reaction products at 40 min after a single addition of CT Topo I, and at 360 min after three successive additions of CT topo I at 0, 120, 240 min are shown in Figure 1. The relaxed topoisomers are the low peaks in the middle between the nicked circle peak on the far left and the peak on the far right, which contains the (unresolved) residual native supercoiled DNAs. When the integrated intensities of the relaxed topoisomer peaks in each gel scan are plotted versus l_{ex}, the envelope of the intensities is always bell-shaped about a central position that generally falls between the two largest relaxed topoisomer peaks, as observed previously (*24*, *30*−*32*). Equation 1 predicts that the relative peak intensities

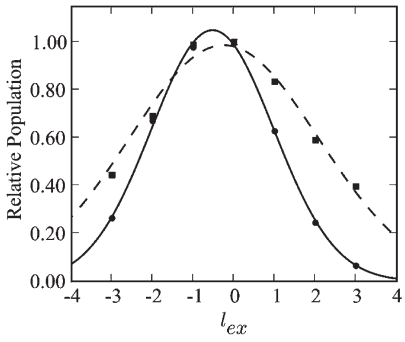

FIGURE 2: Relative population of each topoisomer vs excess linking difference (l_{ex}) for the same two samples shown in Figure 1. The relative population is the ratio of the integrated intensity of a particular peak to that of the largest peak (most populous topoisomer) in the same gel lane, and l_{ex} is the (integral) difference in linking number between the same two species. The curve in each case is the best fit of eq 1 to the observed relative populations for (A) the 40 min sample from Figure 1 (dashed curve); and (B) the 360 min sample from Figure 1 (solid line).

for an equilibrium distribution of topoisomers, when plotted versus l_{ex}, should fall on a Gaussian curve centered at $-\Delta l_0$. For all times of exposure to CT Topo I, the relaxed topoisomer intensity ratios are well fitted by eq 1, as illustrated in Figure 2. The best-fit Δl_0 values (but not the E_T-values) are always the same within the experimental error of ± 0.2 turn! This strongly implies that the visible relaxed topoisomer peaks always constitute an equilibrium distribution with very little or no contribution from intermediate, incompletely relaxed topoisomers. If the latter were present, they would surely have introduced some nonrandom asymmetry into the distribution of peak intensities and caused a significant shift in Δl_0 with increasing time of exposure to active CT Topo I, neither of which was observed.

(2) The linking difference of the most abundant topoisomer under reaction conditions is Δl_0 ($|\Delta l_0| \leq 0.5$), and that remains its linking difference relative to the center of the distribution even in the gel. Gel conditions shift the intrinsic twist, which in turn shifts the linking difference of every relaxed topoisomer, and the center of the distribution, by practically the same amount, δ, relative to that under reaction conditions. The linking difference of the most abundant relaxed topoisomer under gel conditions is then, $\Delta l_0^{gel} = \Delta l_0 + \delta$, and that of any other topoisomer is, $\Delta l^{gel} = \Delta l_0^{gel} + l_{ex}$, where l_{ex} is a small positive integer for peaks immediately to the right of center and a small negative integer for peaks immediately to the left. For the visible relaxed topoisomers, Δl^{gel} extends from ~ 0 (under the nicked circle peak) to $+9$ or $+10$ turns, whereas for the native supercoiled DNAs, Δl^{gel} extends from ~ -12 to -24 turns. No evidence of any incompletely relaxed topoisomers was found either in the gap between the right end of the relaxed topoisomer distribution and the native supercoiled DNA peak, or interposed among the more relaxed topoisomers, for any time of exposure to CT Topo I (in the absence of added ethylene glycol).

(3) The native supercoiled DNA peak always runs at the same position relative to the nicked circles for all times of exposure to active Topo I. This indicates that there is no significant contribution from partial relaxation of topoisomers within that peak to shift it toward the nicked circle peak.

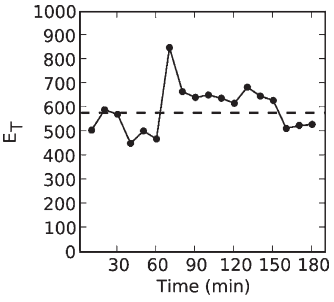

FIGURE 3: E_T vs reaction time for a p30δ sample that received a single addition of 0.1 unit of CT Topo I/μL at $t = 0$ min.

The preceding observations collectively provide compelling evidence that CT Topo I operates in a completely, or almost completely, processive manner to relax the superhelical turns of its currently bound DNA to an equilibrium distribution, before dissociating. Other eukaryotic Topo I enzymes were previously found to act in a largely processive manner under comparable conditions (*33*−*36*). However, neither the equilibrium nature of the resulting distribution, nor the invariance of Δl_0 with time were quantitatively verified.

The complete relaxation of superhelical stress after sufficient exposure to active CT Topo I argues that it is not a type IA topoisomerase, but is consistent with it being a IB topoisomerase (*39*−*41*). The almost completely processive character of the reaction reflects either complete relaxation of superhelical stress in a single cleavage−rotation−religation event, or relaxation via a few successive cleavage−rotation−religation events while bound to the same enzyme. A detailed analysis of the kinetics of the enzyme is presented below. It suggests that on average each complex undergoes 3.34 cleavage and religation events before dissociating. The multiple event scenario is similar to the mechanism suggested for *Vaccinia* type IB topoisomerase, which upon quenching under saturated substrate conditions yielded incompletely relaxed intermediates, as well as completely relaxed products (*35*).

Formation of Metastable Secondary Structure and Its Relaxation by CT Topo I. The temporal trajectory of E_T subsequent to a single addition of CT Topo I is shown in Figure 3. Except for one spurious high value, all of the points lie in the range, $E_T = 580 \pm 130$, which is well below the consensus range for fully equilibrated secondary structure, 1000 ± 100. Moreover, no statistically significant change in E_T occurred over the 180 min time-span of this experiment. About 70% of the original supercoiled DNA is topoisomerized by 120 min, but little or no further topoisomerization occurs from 120 to 180 min (data not shown), indicating that the enzyme is largely or entirely inactive beyond 120 min. The low value of E_T is ascribed to metastable secondary structure in the relaxed topoisomers, which evidently persists for at least 3 h under the prevailing reaction conditions.

In a second experiment, a single solution containing p30δ and CT Topo I, was reacted and sampled for 60 min, at which point it was divided into two aliquots, one of which received a second addition of fresh CT Topo I at that time, and both of which continued to be sampled at 10 min intervals up to 120 min. The temporal trajectories of E_T for this experiment are shown in

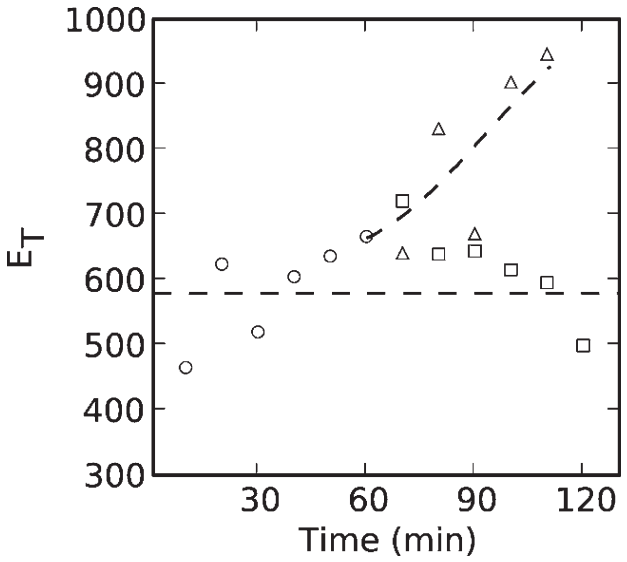

FIGURE 4: E_T vs reaction time for a p30δ sample that received a single addition of 0.1 unit of CT Topo I/μL at t = 0 min, was assayed every 10 min, and was divided into two aliquots at t = 60 min. One aliquot (Δ) received a second addition of 0.1 unit of CT Topo I/μL at t = 60 min and the other ($\square$) did not, and both aliquots continued to be assayed every 10 min up to 120 min. The line and the curve are drawn to guide the eye.

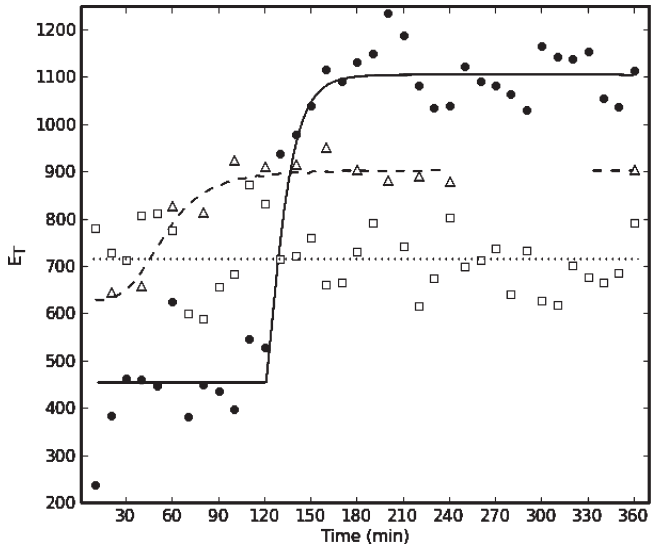

FIGURE 5: E_T vs reaction time for p30δ samples reacted with CT Topo I in different concentrations of ethylene glycol (EG). ($\bullet$) p30δ sample in 0 w/v% EG received three additions of 0.1 unit of CT Topo I/μL at t = 0, 120, and 240 min; (Δ) p30δ sample in 20 w/v% EG received two additions of 0.1 unit of CT Topo I/μL at t = 0 and 120 min; ($\square$) p30δ sample in 40 w/v% EG received three additions of 0.1 unit of CT Topo I/μL at t = 0, 120, and 240 min. Curves are drawn to guide the eye.

Figure 4. The aliquot receiving the second addition of CT Topo I exhibited a subsequent rise of E_T into the consensus equilibrium range, while E_T for the aliquot receiving no fresh CT Topo I remained in the low range, 570 ± 100. The aliquot receiving the second addition of CT Topo I also converted all of its residual supercoiled DNA into topologically relaxed topoisomer peaks, whereas the aliquot receiving only a single addition did not (data not shown). The rise of E_T into the consensus equilibrium range after the second addition of fresh CT Topo I is ascribed to the equilibration of metastable secondary structure by sufficient exposure to active CT Topo I. These results imply that the enzyme becomes inactive within ~60 min. Possible reasons for this loss of activity were noted in Materials and Methods.

In a third experiment, a sample of p30δ received additions of fresh CT Topo I at 0, 120, and 240 min, and was sampled every 10 min up to 360 min. The temporal trajectory of E_T for this experiment is shown as the solid black curve in Figure 5. Again, E_T remains low, largely in the range 450 ± 100, until the second addition of CT Topo I at 120 min, which subsequently elevates E_T to ~1100, in the upper part of the consensus range, 1000 ± 100. This second addition also completes the conversion of the residual supercoiled DNA to topologically relaxed topoisomers by ~150 min (data not shown). The third addition of CT Topo I at 240 min causes no further change in E_T, presumably because any metastable secondary structure has already been equilibrated at earlier times.

Although E_T rises with increasing time of exposure to active CT Topo I, Δl_0 remains constant within the experimental error of ±0.2 turn. This latter finding implies that the intrinsic twist of the metastable secondary structure is practically identical to that of the equilibrium structure under reaction conditions.

The fact that Δl_0 remains constant to within ±0.2 turn throughout the equilibration process suggests that any locally melted regions in the initially formed metastable DNA must collectively comprise at most two base-pairs. Previous simulations of 4349 bp DNAs with 0 and 28 melted bp in 20 mM ionic strength indicate that melting 28 bp reduces the supercoiling free energy by ~22% (*27*), so that melting only 2 bp should reduce the supercoiling free energy by only ~2% or less. For this reason, the possibility that the metastable low value of E_T might arise from elastically soft melted regions is discounted.

An alternative possibility that the initial low value of E_T is attributable in some way to non-catalytic interactions between the DNA and either active or inactive Topo I or its accompanying BSA, is ruled out by two obervations. (1) E_T actually increases into the normal equilibrium range upon further addition of those same proteins. (2) At 120 min, before the second addition of CT Topo I, about 70% of the DNA is relaxed, and the total number of enzyme molecules (active + inactive) per relaxed DNA molecule is (1/58)(1/.70) = 0.025 = 1/40. Under such conditions there is too little enzyme present to affect more than a tiny fraction of the relaxed DNA via non-catalytic interactions.

Another indication that the initially formed secondary structure changes with increasing exposure to active CT Topo I is the following. The gel mobility of any given topoisomer would generally be expected to vary with changes in secondary structure that alter its elastic constants and/or its affinity for chloroquine. Unfortunately, variations in the gels themselves can cause greater differences in mobililty than those due to changes in secondary structure. A 360 min experiment that is sampled every 10 min requires three different gels (12 lanes per gel), one for times from 10 to 120 min, another for times from 130 to 240 min, and a third for times from 250 to 360 min. Although mobility differences between gels are attributable primarily to differences in the gels themselves, systematic changes in mobility within the same gel (due to increasing time of exposure to Topo I) presumably do reflect changes in mobility of the individual topoisomers. In Figure 6 is plotted the average spacing in pixels between peaks of the l_{ex} and l_{ex} −1 topoisomer bands over the span from l_{ex} = −2 to +3 versus time of sampling the experiment. The average peak spacing is just $(x_{+3} - x_{-3})/6$, where $x_{l_{ex}}$ denotes the peak position of the l_{ex} topoisomer in the direction of migration. The data in gels 1 (10−120 min) and 3 (250−360 min) indicate no significant

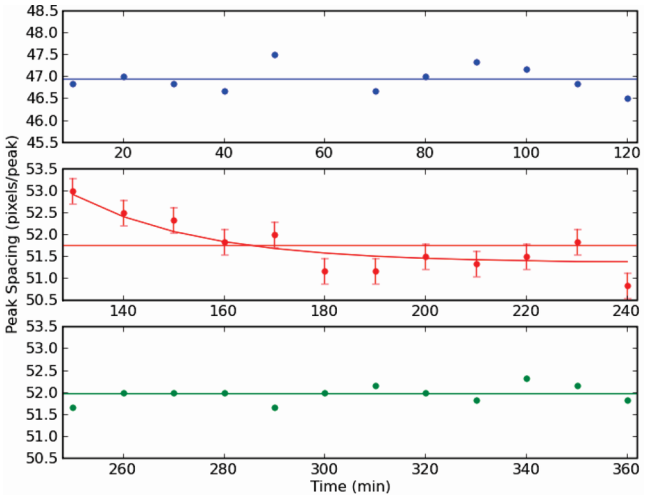

FIGURE 6: Average peak spacing between the seven most populous topoisomers in each gel lane vs time of reaction of p30δ with CT Topo I. The main sample received 3 additions of CT Topo I at 0, 120, and 240 min. Three different gels, each with 12 lanes, were required to analyze all 36 subsamples that were withdrawn for assay (one subsample every 10 min). Differences in mobility of the same species between different gels are generally significant at this level of resolution, so only variations in mobility among subsamples in the *same* gel are considered to be significant. Only the middle gel (130 to 240 min) shows significant variations in average peak spacing among the different subsamples. Best-fit horizontal lines are shown for all three gels and the best-fit exponential plus a preset baseline is shown for the middle gel. The evident decline in average peak spacing from 130 to 180 min is statistically highly significant, as discussed in the text.

decreasing or increasing trend of the average peak spacing with increasing time. However, gel 2 (130−240 min) exhibits an obvious decreasing trend of the data from 130 to 180 min, after which the trend is more or less flat. The data in gels 1 and 3 are well-fitted by horizontal lines, $g(t) = C$, which lie at their respective average values, and their corresponding variances are, $\sigma_1^2 = 0.082$ and $\sigma_3^2 = 0.036$. The variance of the data in gel 2 is assumed conservatively to be the same as the larger of these two estimated values, so $\sigma_2^2 = 0.082$. The data of gel 2 are fitted by the function, $f(t) = A \exp[-kt] + B$, wherein B is fixed at the mean value (51.36) of the points from 190 to 240 min. There is no particular significance to this functional form apart from the fact that it captures the visible trends of the data. The best-fit curve is shown in Figure 6; for that curve, $\chi_f^2 = 11.67$, and the reduced chi-squared is, $\chi_{fr}^2 = \chi_f^2/(12 - 3) = 1.30$. The probability of chi-squared for its 9 degrees of freedom is, $P(\chi^2 > \chi_f^2) = 0.250$, which indicates an acceptable fit of this curve to the data. The same data in gel 2 are also fitted by a horizontal line, $g(t) = C$, and the best-fit horizontal line is shown in Figure 6. For this line, $\chi_g^2 = 53.06$, and the reduced chi-squared is, $\chi_{gr}^2 = \chi_{gr}^2/(12-1) = 4.825$, which is most unsatisfactory. The probability of chi-squared for its 11 degrees of freedom is, $P(\chi^2 > \chi_g^2) = 7 \times 10^{-7}$, which indicates an extremely poor fit to the data. The ratio of the probability (P_f) that the data in gel 2 arise from the best-fit curve, $f(t)$, to the probability (P_g) that they arise from the best-fit horizontal line, $g(t)$, is $P_f/P_g = \exp[-(\chi_f^2 - \chi_g^2)/2] = 9.7 \times 10^8$. These results imply a statistically highly significant decrease in the gel spacing between adjacent topoisomer peaks with increasing time of reaction from 130 to 180 min. This is the same time interval in which E_T rises up to its plateau value.

The possibility that the observed change in gel spacing between 120 and 180 min could be attributed to noncatalytic interactions between the DNA and either active or inactive enzyme or its accompanying BSA is ruled out by several considerations. (1) Active and inactive enzyme, peptide fragments, and BSA were extracted by a mixture of phenol, chloroform, and isoamyl alcohol prior to gel electrophoresis, so those species should have been largely removed. (2) There is no comparable change following the addition of active enzyme at either $t = 0$ or $t = 240$ min. (3) The total number of enzyme molecules (active + inactive) per relaxed DNA molecule from 130 to 240 min is less than or equal to $(2/58)(1/0.70) = 0.05 = 1/20$, which is too small to significantly affect the mobility, in view of the following. (4) The gel mobilities of such large relaxed DNAs in 0.8 w/v% agarose gels are very insensitive to the binding of a single nonreactive protein of the size of Topo I or BSA. Indeed, we are aware of no literature examples, wherein binding of a single such protein to such a large DNA has been detected by an altered gel mobility under similar conditions.

This change in gel spacing is attributed to a change in secondary structure and a consequent change in elastic constants and/or affinity for chloroquine. Unfortunately, experimental data regarding the effects of variations in the twisting and bending elastic constants on the gel mobilities of supercoiled DNAs are lacking, so it is not possible to infer with certainty the nature of the changes in elastic constants from our gel mobility data alone. However, we can suggest a plausible scenario.

First, we note that the difference in gel mobility between the jth and first topoisomers to the right of the nicked circle peak under gel conditions is approximately proportional to the difference, $\Delta l_j^{gel} - \Delta l_1^{gel}$, over the range, $\Delta l_j^{gel} = 1$ to 8, although the peak spacing diminishes slightly with increasing Δl_j^{gel}. The linking difference, $\Delta l_j^{gel} = t_j - l_0 + w_j$, contains contributions from both the excess twist, $t_j - l_0$, and writhe, w_j, but only the latter affects the shape that is sensed by the gel. From many simulations, we know that the average writhe is accurately proportional to the linking difference over the range, $|\Delta l_j| \leq 8$ (*25*−*27*, *42*). It may be inferred that the difference in mobility between the jth and first topoisomers is approximately proportional to the difference in average writhe, $\langle w_j \rangle - \langle w_1 \rangle$. Simulations also indicate that the ratio, $\langle w_j \rangle / \Delta l_j$, increases with the ratio, α/κ_β, of the elastic constants for torsion (α) and bending (κ_β) of the effective springs between successive base-pairs, as one would expect. If the α/κ_β ratio should decline during the equilibration of metastable secondary structure, then the average (positive) writhe of each topoisomer in the gel would diminish, resulting in smaller spans, $x_{+3} - x_{-3}$, and average peak spacing, $(x_{+3} - x_{-3})/6$, for the equilibrated species, as observed.

Subsequent discussion of both equilibrium and early time values of α and E_T, and the implied values of the corresponding bending elastic constant in each case, indicates that the ratio, α/κ_β, declines upon equilibration of metastable secondary structure. In addition, the implied increase in bending rigidity above that of the metastable state would likely diminish the fraction of multiply branched or irregular structures, and enhance the fraction of simple interwound structures, which would likely also significantly increase the gel spacing between topoisomers. Hence the changes in elastic constants between 130 and 180 min are consistent with the observed changes in gel mobility.

The foregoing results imply the following conclusions.

(1) Metastable secondary structure with an anomalously (~0.5-fold) low value of E_T is formed immediately upon

relaxation of native superhelical stress by CT Topo I. In the absence of active enzyme, this metastable structure persists under reaction conditions with little or no change for at least three h, and possibly far longer. Under gel conditions (including added chloroquine) the metastable structure persists for longer than half of the 48 h running time, because complete equilibration in much less time would have erased all differences in mobility between the 130−170 min and 180−240 min samples in gel 2, and slow but nearly complete equilibration during the first 24 h would have caused significant smearing of the topoisomer bands of the more positively supercoiled species, neither of which was observed.

(2) Active CT Topo I catalyzes the equilibration of metastable secondary structure, thereby attaining the equilibrium values of E_T and presumably also of the torsion and bending elastic constants, as well as equilibrium values of the gel mobilities. Neither the presence of metastable secondary structure with an anomalously low E_T, nor the acceleration of its equilibration by active CT Topo I was detected in previously published topoisomerization experiments. Either the reaction products were not examined at early times, but only after a sufficient time of exposure to active CT Topo I to equilibrate any metastable secondary structure, or the E_T values were not extracted from the topoisomer distributions at early times. However, in a manuscript that unfortunately was never published, R. Negri, F. Della Seta, E. Di Mauro, and G. Camilloni demonstrated that the electrophoretic mobility of a particular topoisomer in the presence of ethidium increased with increasing time of exposure to eukaryotic topoisomerase I (personal communication from E. Di Mauro (1989)). This phenomenon was observed only for topoisomers with superhelix densities in the absence of dye in the range, $-0.02 \leq \sigma \leq 0$, and strongly suggests the existence of metastable secondary structure in those DNAs, and its subsequent equilibration by topoisomerase I.

(3) No detectable equilibration of metastable secondary structure occurs until after the second addition of fresh CT Topo I at 60 or 120 min, at which time ~70% of the native supercoiled DNA has been relaxed, yet the equilibration is completed within the next hour, not long after the last supercoiled DNAs are relaxed. In a subsequent section, this temporal lag of the equilibration process behind the relaxation process is suggested to arise not from any equilibrium or kinetic preference of CT Topo I for native supercoiled DNA over relaxed DNA, but instead from a requirement for multiple cleavage and religation events, possibly at different positions on the DNA, in order to facilitate equilibration.

Estimated Elastic Constants of the Equilibrium and Metastable States. Analytical theory plus simulations yield a fairly accurate, approximate relation between E_T on one hand and α and κ_β on the other (*4*, *43*),

$$E_T = ((2\pi)^2/2kT)\alpha B\kappa_\beta/(\alpha + B\kappa_\beta) \quad (2)$$

wherein $B = 0.594$. When E_T and α are known, eq 2 can be solved for κ_β (*43*).

For the equilibrium state, the measured values for the present DNA are $(E_T)_{eq} = 1100$ and $(\alpha)_{eq} = 6.35 \times 10^{-19}$ J, which upon substitution into eq 2 yield, $(\kappa_\beta)_{eq} = 6.43 \times 10^{-19}$ J and $(P)_{eq} = h\kappa_\beta/kT = 51$ nm, where $h = 0.34$ nm is the rise per bp. For the metastable DNA, $(E_T)_m \simeq 533$, but $(\alpha)_m$ was not measured. However, for other supercoiled DNAs, the value of $(\alpha)_m$ prevailing immediately after release of superhelical strain was typically about 0.6 to 0.7 times the equilibrium value (*1*−*8*). For the present DNA, such a reduction would give, $(\alpha)_m = (3.8 \text{ to } 4.4) \times 10^{-19}$ J. Inserting $(E_T)_m$ and $(\alpha)_m$ into eq 2 yields: $(\kappa_\beta)_m = (2.64 \text{ to } 2.80) \times 10^{-19}$ J and $(P)_m$ 21−22 nm. Apparently, the bending elastic constant and associated persistence length of the metastable state are less than half of their corresponding equilibrium values. These elastic constants yield the ratios, $(\alpha/\kappa_\beta)_m = 1.36$ to 1.67 and $(\alpha/\kappa_\beta)_{eq} = 0.99$. Thus, the α/κ_β ratio declines during the equilibration of the metastable state, which should diminish the $wj/\Delta l_j$ ratio and gel spacings, as observed. In this respect, the changes in E_T and average gel spacing over time from 130 to 180 min are mutually consistent.

Kinetics and Processivity of the Enzyme. A proposed kinetic diagram is presented in Figure 7. It differs from the currently accepted model only by the inclusion of descriptors, S_1, S_m, and S_{eq}, to indicate the secondary structures of, respectively, the original native supercoiled state, the metastable relaxed state, and the equilibrium relaxed state, which appears only after continued action of the enzyme. The enzyme first binds to the DNA to form a noncovalent complex, which may then either dissociate or undergo a cleavage reaction. During the cleavage step, a phosphate ester bond of one strand is transferred from the 5′-oxygen of its succeeding furanose ring to the hydroxyl oxygen of a proximal tyrosine of the enzyme (*41*). Thus, the DNA becomes covalently attached to the enzyme on the 3′ side of the cleavage site, and exhibits a free -OH on the 5′ side. The winding/unwinding motion of the free 5′-end around the uncleaved strand is responsible for the net loss of initial superhelical turns. On each cycle past the original cleavage position, there is a finite probability of religation to form a new noncovalent complex with an altered linking difference, $\Delta l_0 \pm n$, $n = 0, \pm 1, \pm 2, \pm 3 \ldots$. After sufficient unwinding of a native supercoiled DNA, there emerges an altered metastable secondary structure, S_m, whose rate of equilibration is evidently accelerated by further cleavage and religation cycles, possibly at different points on the DNA, as discussed below.

The principal question addressed in this section is whether the highly processive behavior of CT Topo I can be quantitatively rationalized by (1) invoking plausible estimates of the relevant kinetic and equilibrium constants, and (2) making use of recent data pertaining to the unwinding of a single twisted DNA under tension, which contains a superhelical pseudocircular domain, in the presence of human Topo I (*36*). In the subsequent discussion, it is assumed that the kinetic constants for CT Topo I are identical to those of human Topo I, and that the equilibrium and kinetic constants for the religation reactions of both CT and human Topo I are identical to those for *Vaccinia* Topo I.

Under conditions where the average number of bound human Topo I molecules per DNA is ≤0.5, for example when the concentrations of both species are less than or comparable to the effective dissociation constant, K_d, it was found (by measuring the relative amounts of complexed and free DNA) that K_d is practically the same for both supercoiled and relaxed DNAs, with a value, $K_d \simeq 0.2$ nM (*37*). A similar value, $K_d \simeq 0.1$ nM, was obtained for supercoiled DNA by a different method (*44*). However, under conditions of high total enzyme concentration

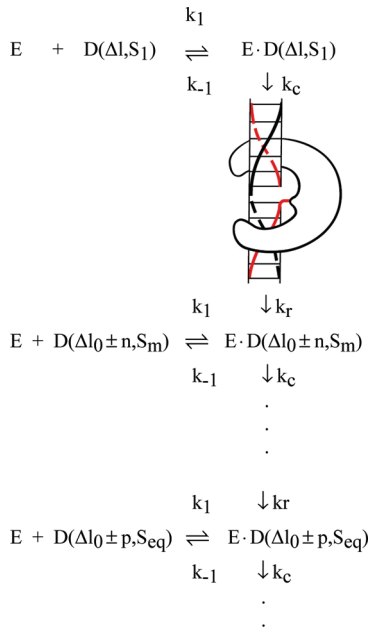

FIGURE 7: Proposed mechanism of CT Topo I. This is identical to the current standard model, except for incorporation of the symbols, S_1, S_m, and S_{eq}, to denote the different helical secondary structures in, respectively, the equilibrium native supercoiled DNA, the long-lived metastable state of a recently relaxed DNA, and the equilibrium state of a relaxed DNA. The novel aspect of this proposed mechanism is the second function of CT Top I to equilibrate the S_m structure of relaxed DNAs via continued cleavage and religation cycles.

($[E]_{tot} \gg K_d$) and moderate or large enzyme excess ($[E]_{tot}/[DNA]_{tot} \geq 1.6$), human Topo I strongly (by ≥10-fold) prefers the supercoiled DNA over the relaxed species at equilibrium (*37*). In an attempt to rationalize these apparently conflicting results, it was suggested that the binding sites of relaxed and supercoiled DNAs have very similar K_d, but are simply much more numerous in supercoiled DNAs (*37*). However, such a model inevitably yields a proportionately greater number of bound Topo I on the supercoiled DNA at the same free enzyme concentration, and also a substantially lower free enzyme concentration at which half of the supercoiled DNAs contain no bound Topo I, contrary to results of the binding experiments (*37*). A plausible alternative explanation would require similar numbers of sites with the very lowest K_d in relaxed and supercoiled species, but considerably more sites with somewhat larger values of their effective K_d in the supercoiled species. Such behavior could arise from an anticooperativity of the binding that is greater in relaxed than in supercoiled DNAs, as described below.

CT Topo I binding to both both modestly supercoiled pBR322 and linear fragments thereof was studied at molar ratios (enzyme/DNA) of 3:1 and 4.3:1, respectively, by electron microscopy. Binding was found to occur predominantly at duplex DNA crossovers (*45*). The distance between the crossing duplex segments at a binding site must be 3.5−4.0 nm in order that the second duplex segment may contact the backside of a Topo I that is bound on its front side (in normal fashion) to the first duplex segment. The probability per unit length for the separation between nearest nonadjacent (along the contour) duplex segments in a simulated native supercoiled ($\sigma = -0.05$) DNA exhibits a sharp maximum at ∼9.0 nm, and an integrated probability of ∼0.02 for separations less than ∼4.0 nm (*46*). In order to stabilize a binding site at an existing crossover, the duplex segments must be forced together, so as to hold their separation near 3.5 to 4.0 nm with probability 1.0. The overall binding site construction process can be accomplished stepwise via: (1) the requisite increase in writhe to generate a crossover, and (2) the compression of the two duplex filaments together to achieve a 3.5−4.0 nm separation with the least amount of work, which occurs for high crossing angles ∼90°. The number of stable crossovers in a circular DNA is assumed to be practically equal to $|w|$.

In a supercoiled DNA with $|\Delta l| \gg 1.0$, the mean writhe, $\langle w \rangle$, and mean excess twist, $\langle t \rangle - l_0$, have the same sign and both have absolute values much greater than 1.0, so the DNA exhibits $|\langle w \rangle| \gg 1.0$ stable crossovers at the outset. However, for a completely relaxed topoisomer, one has $\Delta l = 0$ and initially also $\langle w \rangle = 0$ and $\langle t \rangle - l_0 = 0$. In this case, a change in writhe, $w - \langle w \rangle = \pm 1.0$, is required for each crossover-bound Topo I, and must be accompanied by an *identical change of opposite sign* in $t - \langle t \rangle$ in order to satisfy the topological constraint, $\Delta l = l - l_0 = \langle t \rangle - l_0 + \langle w \rangle = t - l_0 + w =$ constant (*47*, *48*).

The free energy cost to construct a crossover binding site is the sum of costs for the writhing and compression steps. For a crossover complex to be more stable than a noncrossover complex, this cost must be overcompensated by the decrease in electrostatic free energy of the two negatively charged DNAs and the positively charged Topo I and by any decrease in short-range attractive interaction energy between the second duplex segment and the backside of the Topo I, relative to their corresponding values prior to binding.

The free energy, or work, to increase the magnitude of the writhe (w) above that of the mean value, $\langle w \rangle$, at constant Δl (in the absence of Topo I), is just the potential of mean force associated with such a fluctuation in writhe, which is given by eq (A14) of ref *4*,

$$U(w - \langle w \rangle) = ((\alpha + B\kappa_\beta)/2N)(2\pi)^2(w - \langle w \rangle)^2 \qquad (3)$$

where $\langle w \rangle = (\alpha/(\alpha + B\kappa_\beta))\Delta l$ is an approximate expression for the mean writhe. If the number of crossovers needed for binding sites is $|w|$, and $|w| < |\langle w \rangle|$, then the writhe requirement is already satisfied, and no work is required for this step. If the number of crossovers needed is $|w|$, and $|w| > |\langle w \rangle|$, then the work to increase the magnitude of the writhe from $|\langle w \rangle|$ to $|w|$ is given by eq 3. For a completely relaxed topoisomer containing 4500 bp with $\Delta l = 0 = |\langle w \rangle|$, the first crossover requires, $w = \pm 1.0$, so $|w - \langle w \rangle| = 1.0$. For typical values, $\alpha = 6.0 \times 10^{-19}$ J, $\kappa_\beta = 6.3 \times 10^{-19}$ J, and $B = 0.594$, eq 3 yields, $U(1.0) = (1.0)kT$ at 310 K. For a topoisomer with $|\Delta l| = 1.0$, the mean writhe is approximately, $\langle w \rangle = 0.62$. The first crossover again requires, $w = 1.0$, so $|w - \langle w \rangle| = 0.38$, and $U(0.38) = (0.14)kT$. For all topoisomers with $|\Delta l| \geq 2.0$, one has $|\langle w \rangle| > 1.0$, and no writhe work is required to create the first crossover. Thus, the cost of the writhe step for the first crossover is significant for $\Delta l = 0$, considerably smaller for $|\Delta l| = 1.0$, and negligible for all higher values of Δl. For the same DNA, the free energy cost of an additional crossover to create an excess writhe, $\langle w - \langle w \rangle \rangle = n + 1$, beginning with an excess writhe, $\langle w - \langle w \rangle \rangle = n$, is given by, $U(n + 1) - U(n) = kT(1 + 2n)$ at 310 K. Thus, the cost of each additional writhe turn in excess of $|\langle w \rangle|$ rises linearly with the number of excess writhe turns. Consequently, the writhe cost to achieve multiple binding sites is much greater in topoisomers with small $|\Delta l|$, which require more excess writhe turns to achieve the same total number of sites.

The free energy cost to compress the first crossover into a binding site is expected to rise somewhat with increasing $|\Delta l|$, because it is the cost of imposing an additional constraint on an

increasingly constrained and less compliant system. For that same reason, the compression cost of each subsequent binding site at a given $|\Delta l|$ is also expected to rise with the number of sites already created.

Within these guidelines, it is possible that: (1) the total free energy cost of the first binding site in a native supercoiled DNA contributes a factor to the overall binding constant ($K_a = 1/K_d$) that is comparable to the population weighted average of such factors for the topoisomers, $\Delta l = 0, \pm 1.0, \pm 2.0, \pm 3.0...$; and (2) the K_a values for subsequent binding sites at a given Δl fall increasingly far below that of the first site, and they fall farther for smaller $|\Delta l|$. Hence, this scenario could potentially account for both the similar binding of Topo I to supercoiled and relaxed DNAs at very low binding levels, and the much greater preference of Topo I for supercoiled DNAs at higher binding levels. It also predicts that the binding constant for the first Topo I bound to the $\Delta l = 0$ topoisomer should be lower than those for the other relaxed topoisomers by a factor, $\sim\exp[-1.0] = 0.37$ or less, for a 4500 bp DNA at 310 K, and by a factor, $\sim\exp[-2.0] = 0.13$ or less, for a 2250 bp DNA. This effect might be at least partly responsible for the reported singularly low reactivity of the $\Delta l = 0$ topoisomer with various eukaryotic type I topoisomerases at low binding levels under low salt (irreversible binding) (*49*) or under high salt plus camptothecin (*50*) conditions. This effect agrees qualitatively with the conclusion that the "availability" of reactive binding sites is significantly lower in the $\Delta l = 0$ topoisomer than in other relaxed topoisomers (*51*).

Electron and atomic force microscopy studies at higher $[E]_{tot}/[DNA]_{tot}$ ratios (10 to 60) revealed cooperative binding to linear, nicked circular, and relaxed circular DNAs to produce filaments, wherein two duplex DNA segments are synapsed and in simultaneous contact with many *Vaccinia* Topo I molecules along the length of the synapsed region (*52*, *53*). This raises the possibility that cooperative interactions between neighboring bound Topo I molecules might be important (*53*). However, a recent study of the preference of human Topo I for supercoiled DNAs effectively ruled out protein:protein association either when free in solution or bound to short duplex DNAs (*54*). A mutational analysis traced the preference for supercoiled substrates to the coiled-coil linker region, which contains six lysines, and to four solvent exposed lysines on the backside of core subdomain III (*54*). This suggests that the stabilization of crossover binding sites is largely electrostatic.

The cooperative binding and intramolecular synapsis and filament formation likely arise primarily from combined electrostatic interactions and DNA elastic forces. Simulations and analytical theory for negatively charged semiflexible filaments interacting with smaller multivalent cations, which have no intrinsic tendency to associate, predict cooperative cation-induced synapsis of two filaments (or two segments of the same filament) and intramolecular bundle formation (*54*−*57*). The cooperativity results from the initial preference of two DNA segments to cross at right angles with only one or a few multivalent cations bridging the junction (*55*−*57*). Increasing the concentration of multivalent cations induces a cooperative transition to a parallel configuration with many bridging cations distributed along the length of the synapsed region (*55*−*57*).

The microscopy evidence suggests that cooperative Topo I binding does not occur at low to moderate ratios, $[E]_{tot}/[DNA]_{tot} \leq 3.0$, and provides no indication that the cooperative binding observed at higher ratios, $[E]_{tot}/[DNA]_{tot} \geq 10$, actually occurs preferentially on supercoiled rather than relaxed substrates. Thus, the increasing preference of Topo I for supercoiled DNA with increasing binding level up to moderate ratios, $[E]_{tot}/[DNA]_{tot} \leq 1.6$, is more likely to arise from the greater anticooperativity of Topo I binding to more relaxed topoisomers, as discussed above, than to a greater cooperativity of Topo I binding to more supercoiled molecules.

In any case, this study is carried out in large excess of DNA, $[E]_{tot}/[DNA]_{tot} \leq 0.053$, so multiple Topo I binding should not occur, and no preference of the enzyme for supercoiled over relaxed DNA is expected.

The rate constant for dissociation of human Topo I from relaxed DNA under conditions of high enzyme concentration ($[E]_{tot} \gg K_d$ and $[E]_{tot}/[DNA]_{tot} \geq 1.6$) was reported to be, $k_{-1} = 0.06\ s^{-1}$, and that for dissociation from the corresponding supercoiled DNA was found to be similar (*37*). Given their similar values of K_d and k_{-1}, the association rate constants, k_1, of supercoiled and relaxed DNAs are expected to be also rather similar. Under the present conditions of excess substrate, where only sites with the very lowest K_d are occupied, the value of k_{-1} should be the same as or smaller than, $0.06\ s^{-1}$. This is so, because the forward rate constant, $k_1 = 3.0 \times 10^8\ M^{-1}\ s^{-1}$, is so large as to be diffusion-limited (after accounting for orientational constraints), and could not be further increased. Hence, the lowest value of K_d must be associated with the lowest value of k_{-1}.

The reported equilibrium constant for the cleavage and religation reaction was, $K_c = 0.075$, for *Vaccinia* Topo I acting on supercoiled pUC19 DNA (*35*). A value for the religation rate constant can be reckoned from single-molecule studies of *Vaccinia* Topo I acting on a twisted half-length λ DNA under tension (*36*). The reported probability of religation per turn is, $p_r = k_r/(\langle \dot{n} \rangle + k_r) = 0.03$, where $\langle \dot{n} \rangle$ is the average rate of unwinding (turn s^{-1}) in the cleaved covalent complex. We have analyzed the reported equilibrium and dynamic data (36) to estimate $\langle \dot{n} \rangle$ (J. M. Schurr and B. S. Fujimoto, Ms. in preparation). First, E_T was determined for the superhelical pseudocircular domain(s) of this DNA, which is held at equilibrium under 0.2 pN tension, by means of new theory developed for that purpose. This value of E_T was then used to analyze the dynamic unwinding and extension data in the presence of *Vaccinia* Topo I. The tension experienced by the DNA was assumed to be the magnetic force minus the (significant) hydrodynamic drag force on the translating bead to which the DNA was tethered (*58*). In addition, the DNA tertiary structure was assumed to equilibrate so rapidly as to maintain equilibrium throughout the dynamic unwinding and extension process. Justification for this latter assumption comes from a study of the rates of DNA response (extension) to sudden decreases in force and to the action of nicking enzymes (*58*). Under this assumption, the friction opposing the unwinding (distinct from that opposing the bead motion) arises entirely from the interaction of the rotating DNA with the enzyme. Our analysis of the mean rate of extension of a covalent complex of DNA with *Vaccinia* Topo I yielded, $\langle \dot{n} \rangle = 85.4$ turn s^{-1}, which together with p_r yields, $k_r = 2.6\ s^{-1}$ and $t_r = 1/k_r = 0.38$ s. From the values of K_c and k_r we also estimate the cleavage rate constant, $k_c \simeq 0.20\ s^{-1}$, and average lifetime, $t_c = 5.0$ s. The average time per cleavage and religation cycle is, $t_{cr} = t_c + t_r = 5.4$ s. The time for rotation (winding or unwinding) is omitted, because the "clocks" for rotation and religation run concurrently. The average number of cleavage and religation cycles per binding and dissociation event is reckoned as follows. The "clocks" for dissociation and cleavage run concurrently and stop at the moment of each cleavage step. They resume after each religation step, and continue in this manner until dissociation occurs. Thus,

the average number of cleavage and religation cycles (n_{cr}) before the complex dissociates is just the ratio of the average times for these concurrent steps, $n_{cr} = t_{diss}/t_c = (1/k_{-1})/(1/k_r) = (16.7)/(5.0) = 3.34$. This value should be a lower bound, since the value, $k_{-1} = 0.06\ s^{-1}$, is an upper bound as noted above. Although the religation and cleavage rate constants obtained above are 0.65-fold smaller than those reported by Stivers et al. (*35*), they are favored here for two reasons. (1) Under the substrate-saturated conditions employed by Stivers et al., a fraction of the DNAs may have bound two (or more) enzyme molecules simultaneously. (2) In the kinetic model used to analyze the data, the rate constant for unwinding was assumed to be independent of the torque, or superhelix density, which is now known to be incorrect. Either or both of these problems might have introduced significant error into the best-fit parameters.

We now estimate how far a supercoiled DNA is relaxed in the course of a single binding and dissociation event, which on average consists of 3.34 cleavage and religation cycles, that on average provide (3.34)(0.38) = 1.27 s of unwinding time. In a covalent complex of CT Topo I with a circular superhelical DNA, the unwinding/winding motion of the free 5′-end around the uncleaved strand can be regarded as overdamped thermal Brownian motion in a harmonic potential well along the winding coordinate (($\phi \equiv 2\pi\Delta l_0$)), because the supercoiling free energy varies practically quadratically with ϕ. The origin of the winding angle, $\phi = 0.0$, is taken at the minimum of the potential well, which does not generally correspond to any of the positions, $\phi = 2\pi(\Delta l_0 \pm n)$, $n = 0, \pm 1, \pm 2, 3, ...$, where religation to form a covalently closed topoisomer in a noncovalent complex is possible. When the torque constant and friction factor for the motion are constant in time, the probability density for ϕ at any time, given that $\phi = \phi_0$ at $t = 0$, is given by

$$P(\phi, t|\phi_0, 0) = \exp\left[-\left(\frac{(\phi - \phi_0 e^{-t/\tau})^2}{2(kT/g)(1-e^{-2t/\tau})}\right)\right] / (2\pi(kT/g)(1-e^{-2t/\tau}))^{1/2} \quad (4)$$

wherein $g = 2kTE_T/(N(2\pi)^2)$ is the (known) torque constant, and the unwinding rate constant is, $1/\tau = g/f$, where f is the friction factor for the motion (*59*). In an analysis of data pertaining to the unwinding of a single, twisted, half-length λ DNA held under tension in the presence of human Topo I (*36*), both the torque and rate of unwinding were reckoned. The value obtained for the torque during the unwinding was less than half of that estimated by Koster et al. (*36*), which was inaccurate for reasons discussed elsewhere (J. M. Schurr and B. S. Fujimoto, Ms. in preparation). From the torque and angular velocity, the friction factor was calculated to be, $f = 1.01 \times 10^{-23}\ J\ rad^{-1}\ s$. By using the equilibrium value, $E_T = 1100$, found for the present p30δ, we estimate, $g = 4.84 \times 10^{-23}$ J, and finally $\tau = 0.209$ s. In the 1.27 s of total unwinding time during an average binding and dissociation event, there are 1.27/0.209 = 6.08 relaxation times (τ). Because exp[−6.08] = 0.0023, this total unwinding time suffices to erase virtually all memory of the initial ϕ_0 values and practically attain the equilibrium distribution of topoisomers. This result is in harmony with the observed almost completely processive character of the topoisomer relaxation.

In a single cleavage and religation cycle, there are 0.38/0.209 = 1.8 relaxation times, and exp[−1.8] = 0.16, so relaxation of the average winding angle, $\langle\phi\rangle = \phi_0 e^{-t/\tau}$, has already progressed rather far, for example from −24 turns ($\sigma = -0.05$) to −3.8 turns ($\sigma = -0.008$), where metastable secondary structure is expected to prevail in most of the visible topoisomers in any case. It may be inferred that the enzyme on average spends more time bound to largely relaxed DNA than to native supercoiled DNA throughout the topoisomerization process, even during its very first encounter with a native supercoiled DNA. After one cleavage and religation cycle, about half of the visible topoisomers lie within the typical equilibrium range, $l_{ex} = -3$ to +3, and on average the CT Topo I remains attached to that same DNA for another 2.34 cleavage and religation cycles before dissociating. Thus, the lag in equilibration of metastable secondary structure behind the topoisomerization process cannot be ascribed to insufficient contact of the enzyme with relaxed topoisomers during the early and middle stages of the overall reaction. Instead, it appears that more cleavage and religation cycles, possibly at different sites on the DNA, may be required to accelerate the equilibration of metastable secondary structure.

Do Multiple Nicks in a Relaxed Supercoiled DNA Accelerate Equilibration of Its Metastable Secondary Structure? An indication that multiple nicks might accelerate the equilibration of metastable secondary structure is found in the following observations. After linearization by *Eco*RI, which cuts at a single site, the molar ellipticity of a (formerly) supercoiled ColE1 amp DNA was found to be, $[\theta]_{270} = 5800$, well below the expected low-salt equilibrium value, $[\theta]^{eq}_{270} = 7585 - 7750$ (*60*). However, when the same supercoiled DNA was (multiply) nicked by DNase I, it remained a circular DNA (without superhelical strain), and its molar ellipticity was, $[\theta]_{270} = 7300$, much closer to the equilibrium value (*60*). This would be consistent with a model requiring multiple nicks, either transient or permanent, to equilibrate the metastable secondary structure.

How might single-strand nicks act to equilibrate metastable secondary structure of duplex DNA? As discussed elsewhere, numerous observations suggest that the transitions between at least some conformational substates of duplex DNA are highly cooperative with average domain sizes ranging from lower bound values of 30 to 50 bp up to estimates of 300−500 bp in some cases (*1*−*3*, *9*−*12*, *30*, *32*). This high cooperativity is ascribed to a large free energy associated with junctions between domains of different structure. Equilibration of metastable secondary structure proceeds in large part by the net migration of $S_m|S_{eq}$ and $S_{eq}|S_m$ junctions in the direction of the less stable S_m domain. However, the junction free energy most likely varies significantly with position along the sequence, and junctions may become trapped at certain particularly stable positions. We speculate that the release of local backbone constraints by nicking may help to diminish the junction free energy and/or its variation with position, and thereby release the junction from its trap, so that equilibration can proceed in a more facile manner.

Significance. The practical significance of these observations is 2-fold. First, exposure to active CT Topo I provides a means to accelerate the equilibration of metastable secondary structure, which should improve the reliability and reproducibility of structure-sensitive measurements on DNAs that have recently undergone significant changes in superhelical stress. Conceivably, it could also accelerate the equilibration of metastable secondary structure subsequent to other kinds of perturbations. Second, this activity of such a topoisomerase I enzyme should provide cells a means to equilibrate any metastable duplex secondary structure that results from variations in superhelical

stress during the course of their normal biological activities, such as transcription and replication.

The fundamental significance of these observations is that they provide additional evidence for the metastable duplex state, S_m, that appears initially upon relaxation of superhelical stress. The existence of such a state necessarily implies that the S_1 secondary structure, which prevails over much of all of the sequence in a native supercoiled DNA, differs from the S_{eq} state of a relaxed DNA in some way that is more profound than a simple deformation within a single-minimum basin of the potential-of-mean-force. That is, S_1 and S_{eq} must be associated with different basins with different minima in the potential-of-mean-force (as a function of Δl). Moreover, the S_1 and S_{eq} basins are most likely separated by two barriers and an intermediate basin corresponding to the S_m state. When Δl is varied quickly from a native value, corresponding to $\sigma = -0.05$, to a sufficiently low value corresponding to $\sigma \leq -0.015$, much or all of the sequence becomes kinetically trapped in the S_m state.

Effects of Ethylene Glycol. In 20 w/v% ethylene glycol (EG), partially relaxed topoisomers become visible at early times in the gap between the native supercoiled DNA peak and the peaks of the completely relaxed topoisomers (data not shown). However, the intensities of the completely relaxed topoisomers significantly exceed those of the partially relaxed species. Evidently, 20 w/v% EG diminishes, but does not eliminate, the processivity of CT Topo I in its relaxation of superhelical strain.

The temporal trajectory of E_T in 20 w/v% EG is shown by the dashed line in Figure 5. It rises from a low value, $E_T \sim 630$, at 20 min to a plateau value, $E_T \sim 900$, at about 100 min, before a second addition of CT Topo I at 120 min, which causes no further change. The low values at early times are again attributed to metastable secondary structure in the relaxed toposiomers. The plateau value of E_T for $t > 100$ min corresponds to its equilibrium value, as shown by the following experiment.

A DNA sample in 20 w/v% EG received only a single addition of CT Topo I at $t = 0$. The temporal trajectories of E_T for this and the previous sample are shown in Figure 8, and are within experimental error identical to each other. The second addition of CT Topo I clearly has no effect on E_T, which implies that the metastable secondary structure has equilibrated within ~100 min after a single addition of CT Topo I.

A significant fraction of the DNA remains in the native supercoiled peak at 240 min in the sample that received only a single addition of Topo I, whereas the sample that received a second addition of CT Topo I at 120 min converted all of its native supercoiled peak to relaxed topoisomers (data not shown). These results indicate that CT Topo I activity to relax superhelical stress in 20 w/v% EG dies within 120 min.

The fraction of residual DNA in the native supercoiled peak at 120 min in 20 w/v% EG is less than in the absence of EG (data not shown). Evidently, CT Topo I activity to relax superhelical stress in 20 w/v% EG is either greater, or dies less rapidly, than that in 0 w/v% EG. Metastable secondary structure is equilibrated much more rapidly in 20 w/v% than in 0 w/v% EG. Moreover, the relative enhancement of the rate by 20 w/v% EG appears to be much greater for equilibration of metastable secondary structure than for relaxation of superhelical stress. This suggests that EG might directly catalyze the equilibration of metastable secondary structure in parallel with the action of CT Topo I.

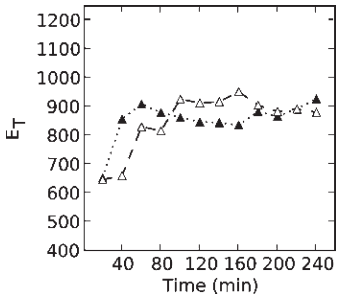

FIGURE 8: E_T vs reaction time in 20 w/v% EG for two p30δ samples. Open triangles (Δ) denote the p30δ sample that received two additions of 0.1 unit of CT Topo I/μL at $t = 0$ and 120 min. These are the same data displayed displayed also as Δ in Figure 5. Filled triangles pertain to a p30δ sample that received a single addition of 0.1 unit of CT Topo I/μL at $t = 0$ min. These two data sets agree within experimental uncertainty. Evidently, the second addition of CT Topo I has no significant effect, and the metastable secondary structure is already equilibrated within ~60 min.

In 40 w/v% EG, the relative intensity of partially relaxed topoisomers in the gap is significantly greater than in 20 w/v% EG (data not shown), so the processivity of Topo I is evidently reduced still further, but not entirely eliminated.

The temporal trajectory of E_T in 40 w/v% EG is also shown in Figure 5. This sample received additions of Topo I at $t = 0$, 120, and 240 min. Within experimental error E_T remains constant over time. There is no evidence of metastable secondary structure at the shortest times examined. The equilibrium plateau value of E_T in 40 w/v% EG lies about as far below that in 20 w/v% EG, as the latter lies below that in 0 w/v% EG. This is precisely the order expected from the recently reported reverse sigmoidal (equilibrium) transition induced by EG, the midpoint of which lies close to 20 w/v% EG (*30*).

These observations suggest and are consistent with the following scenario. Prior to addition of CT Topo I, the native supercoiled DNA is pre-equilibrated with the added EG. It is assumed that the extent of supercoiling does not significantly affect the ability of EG to induce the alternative structure (S_{EG}). Then in 20 w/v% EG, near the midpoint of the transition, about half of the native supercoiled DNA sequence should exist as the normal conformer, S_1, and half as the S_{EG} conformer (*30*). In 40 w/v% EG, practically the entire sequence of the native supercoiled DNA should be in the S_{EG} state. Upon relaxation of the superhelical stress, the S_1 conformer evolves to form the metastable state, S_m, but the S_{EG} conformer does not evolve at all. The effective initial E_T-value for a DNA with half of its sequence in the S_m state and half in the S_{EG} state is related to the E_T-values of those two states by, $1/E_{T_i} = (0.5)(1/E_{T_m} + 1/E_{T_{EG}})$, where $E_{T_m} = 533 \pm 60$ is taken as the average of the observed values ($E_{T_m} =$ 580,570,450) for the S_m state in 0 w/v% EG, and $E_{T_{EG}} = 720 \pm 12$ is the average value for the S_{EG} state in 40 w/v% EG, as inferred from Figure 5. All stated uncertainties are standard deviations of the mean, which are estimated by assuming that the standard deviations of the individual E_T-data points are ~70 in all cases. The calculated initial value, $E_{T_i} = 613 \pm 34$, and the observed initial value, $E_{T_i}^{obs} = 630 \pm 49$, for 20 w/v% EG agree well within the statistical uncertainty of either value. Similarly, the effective final value for a DNA with half its sequence in the S_{eq} state and half in the S_{EG} state is related to the E_T-values of those two states by, $1/E_{T_f} = (0.5)(1/E_{T_{eq}} + 1/E_{T_{EG}})$, where $E_{T_{eq}} \simeq 1100 \pm 15$ is the average value for the S_{eq} state. The calculated final value,

E_{T_f} = 870 ± 13, for 20 w/v% EG agrees with the observed plateau value, $E_{T_f}^{obs} \simeq$ 900 ± 23, within their combined uncertainties ($\sigma_{E_{Tf}} + \sigma_{E_{Tf}}^{obs} = 36$).

In 40 w/v% EG, the EG-induced conformer predominates throughout, so the effective E_T-value should remain constant over time at $E_{T_{EG}} \simeq 720$, as observed in Figure 5. This proposed scenario is the simplest model that is quantitatively consistent with all of the E_T-data.

Significance of the EG Results. The effects of EG provide evidence that the alternative duplex state, S_{EG}, whose relative population increases with w/v% EG, differs not only from the equilibrium state, S_{eq}, of a relaxed DNA in 0 w/v% EG, but also from the metastable state, S_m, that is formed from the S_1 state upon relaxation of the initial native superhelical stress. The S_{EG} state exhibits no long-lived metastable state upon release of superhelical stress. The present studies strongly suggest that the S_m and S_{EG} states coexist in the same topologically relaxed samples at t = 0, and that during the equilibration process the S_{EG} state coexists with both the S_m and S_{eq} states, until all of the S_m state is converted to S_{eq}.

REFERENCES

1. Shibata, J. H., Wilcoxon, J., Schurr, J. M., and Knauf, V. A. (1984) Structures and dynamics of a supercoiled DNA. *Biochemistry 23*, 1188–1194.
2. Song, L., Fujimoto, B. S., Wu, P.-G., Thomas, J. C., Shibata, J. H., and Schurr, J. M. (1990) Evidence for allosteric transitions in secondary structure induced by superhelical stress. *J. Mol. Biol. 214*, 307–326.
3. Schurr, J. M., Fujimoto, B. S., Wu, P.-G., Song, L. (1992) Fluorescence studies of nucleic acids: dynamics, rigidities, and structures, in Topics in Fluorescence Spectroscopy, Vol. 3: Biochemical Applications (J. R. Lakowicz, Ed.) pp 137−229, Plenum Press, New York.
4. Wu, P.-G., Song, L., Clendenning, J. B., Fujimoto, B. S., Benight, A. S., and Schurr, J. M. (1988) Interaction of chloroquine with linear and supercoiled DNAs. Effect on the torsional dynamics, rigidity, and twist energy parameter. *Biochemistry 27*, 8128–8144.
5. Wu, P. G., and Schurr, J. M. (1989) Effects of chloroquine on the torsional dynamics and rigidities of linear and supercoiled DNAs at low ionic strength. *Biopolymers 28*, 1695–1703.
6. Wu, P. G., Fujimoto, B. S., Song, L., and Schurr, J. M. (1991) Effect of ethidium on the torsion constants of linear and supercoiled DNAs. *Biophys. Chem. 41*, 547–565.
7. Naimushin, A. N., Clendenning, J. B., Kim, U.-S., Song, L., Fujimoto, B. S., Stewart, D. W., and Schurr, J. M. (1994) Effect of ethidium binding and superhelix density on the supercoiling free energy and torsion constant of pBR322 DNA. *Biophys. Chem. 52*, 219–226.
8. Langowski, J., Benight, A. S., Fujimoto, B. S., Schurr, J. M., and Schomburg, U. (1985) Change of conformation and internal dynamics of supercoiled DNA upon binding of *E. coli* single-strand binding protein. *Biochemistry 24*, 4044–4028.
9. Kim, U.-S., Fujimoto, B. S., Furlong, C. E., Sundstrom, J. A., Humbert, R. A., Teller, D. C., and Schurr, J. M. (1993) Dynamics and structures of DNA: Long-range effects of a 16 base-pair $(CG)_8$ sequence on secondary structure. *Biopolymers 33*, 1725–1745.
10. Schurr, J. M., Delrow, J. J., Fujimoto, B. S., and Benight, A. S. (1997) The question of long-range allosteric transitions in DNA. *Biopolymers 44*, 283–308.
11. Fujimoto, B. S., Brewood, G. P., and Schurr, J. M. (2006) Torsional rigidities of weakly strained DNAs. *Biophys. J. 91*, 4166–4179.
12. Naimushin, A. N., Fujimoto, B. S., and Schurr, J. M. (2000) Dynamic bending rigidity of a 200 bp DNA in 4 mM ionic strength. *Biophys. J. 78*, 1498–1518.
13. Hustedt, E. J., Spaltenstein, A., Kirchner, J. J., Hopkins, P. B., and Robinson, B. H. (1993) Motions of short DNA duplexes: an analysis of DNA dynamics using an EPR-active probe. *Biochemistry 32*, 1774–1787.
14. Okonogi, T. M., Reese, A. W., Alley, S. C., Hopkins, P. B., and Robinson, B. H. (1999) Flexibility of duplex DNA on the submicrosecond timescale. *Biophys. J. 77*, 3256–3276.
15. Okonogi, T. M., Alley, S. C., Reese, A. W., Hopkins, P. B., and Robinson, B. H. (2000) Sequence-dependent dynamics of duplex DNA: the applicability of a dinucleotide model. *Biophys. J. 78*, 2560–2571.
16. Vologodskaia, M., and Vologodskii, A. (2002) Contribution of the intrinsic curvature to measured DNA persistence length. *J. Mol. Biol. 317*, 205–213.
17. Bauer, W., and Vinograd, J. (1970) Interaction of closed circular DNA with intercalative dyes. II. The free energy of superhelix formation in SV40 DNA. *J. Mol. Biol. 47*, 419–435.
18. Hsieh, T. S., and Wang, J. C. (1975) Thermodynamic properties of superhelical DNAs. *Biochemistry 14*, 527–535.
19. Hinton, D. M., and Bode, V. C. (1975) Ethidium binding affinity of circular lambda deoxyribonucleic acid determined fluorometrically. *J. Biol. Chem. 250*, 1061–1070.
20. Depew, R. E., and Wang, J. C. (1984) Conformational fluctuations of DNA helix. *Proc. Natl. Acad. Sci. U.S.A. 72*, 4275–4279.
21. Pulleyblank, D. E., Shure, M., Tang, D., Vinograd, J., and Vosberg, H. P. (1975) Action of nicking-closing enzyme on supercoiled and nonsupercoiled closed circular DNA: formation of a Boltzmann distribution of topological isomers. *Proc. Natl. Acad. Sci. U.S.A. 72*, 4280–4284.
22. Shore, D., and Baldwin, R. L. (1983) Energetics of DNA twisting. II. Topoisomer analysis. *J. Mol. Biol. 170*, 983–1007.
23. Horowitz, D., and Wang, J. C. (1984) Torsional rigidity of DNA and length dependence of the free energy of DNA supercoiling. *J. Mol. Biol. 173*, 75–91.
24. Clendenning, J. B., Naimushin, A. N., Fujimoto, B. S., Stewart, D. W., and Schurr, J. M. (1994) Effect of ethidium binding and superhelix density on the supercoiling free energy and torsion and bending constants of p30δ DNA. *Biophys. Chem. 52*, 191–218.
25. Gebe, J. A., Allison, S. A., Clendenning, J. B., and Schurr, J. M. (1995) Monte Carlo simulations of supercoiling free energies for unknotted and trefoil knotted DNAs. *Biophys. J. 68*, 619–633.
26. Delrow, J. J., Heath, P. J., and Schurr, J. M. (1997) On the origin of the temperature dependence of the supercoiling free energy. *Biophys. J. 73*, 2688–2701.
27. Sucato, C. A., Rangel, D. P., Aspleaf, D., Fujimoto, B. S., and Schurr, J. M. (2004) Monte Carlo simulations of locally melted supercoiled DNAs in 20 mM ionic strength. *Biophys. J. 86*, 3079–3096.
28. Gebe, J. A., Delrow, J. J., Heath, P. J., Fujimoto, B. S., Stewart, D. W., and Schurr, J. M. (1996) Effects of Na^+ and Mg^{2+} on the structures of supercoiled DNAs: Comparison of simulations with experiments. *J. Mol. Biol. 262*, 105–128.
29. Rangel, D. P., Brewood, G. P., Fujimoto, B. S., and Schurr, J. M. (2007) Effects of ethylene glycol on the torsion elastic constant and hydrodynamic radius of p30δ DNA. *Biopolymers 85*, 222–232.
30. Brewood, G. P., Aliwarga, T., and Schurr, J. M. (2008) A structural transition induced in duplex DNA by ethylene glycol. *J. Phys. Chem. B 112*, 13367–13380.
31. Brewood, G. P. (2006) DNA studies: A novel structural transition, relaxation of secondary structure by Topo I, and resolution of a PCR problem. Ph.D. Thesis, University of Washington.
32. Rangel, D. P., Sucato, C. A., Spink, C. H., Fujimoto, B. S., and Schurr, J. M. (2004) Effects of small neutral osmolytes on the supercoiling free energy and intrinsic twist of p30δ DNA. *Biopolymers 75*, 291–313.
33. McConaughy, B. L., Young, L. S., and Champoux, J. J. (1981) The effect of salt on binding of the eukaryotic DNA nicking-closing enzyme to DNA and chromatin. *Biochim. Biophys. Acta 655*, 1–8.
34. Frølich, R. F., Velgaard, C., Andersen, F. F., McClendon, A. K., Gentry, A. C., Andersen, A. H., Osheroff, N., Stevnsner, T., and Knudsen, B. R. (2007) Tryptophan-205 of human topoisomerase I is essential for camptothecin inhibition of negative but not positive supercoil removal. *Nucleic Acids Res. 35*, 8170–8180.
35. Stivers, J. T., Harris, T. K., and Mildvan, A. S. (1997) *Vaccinia* DNA topoisomerase I: evidence supporting a free rotation mechanism for DNA supercoil relaxation. *Biochemistry 36*, 5217–5222.
36. Koster, D. A., Croquette, V., Dekker, N. H., Shuman, S., and Dekker, N. H. (2005) Friction and torque govern the relaxation of DNA supercoils by eukaryotic topoisomerase IB. *Nature 434*, 671–674.
37. Madden, K. R., Stewart, L., and Champoux, J. J. (1995) Preferential binding of human topoisomerase I to superhelical DNA. *EMBO J. 14*, 5399–5409.
38. Di Mauro, E., Caserta, M., Negri, R., and Carnevali, F. (1985) Activation of *in vitro* transcription and topology of closed DNA domains. *J. Biol. Chem. 260*, 152–159.
39. Champoux, J. J. (2002) Type 1A DNA topoisomerases: strictly one step at a time. *Proc. Natl. Acad. Sci. U.S.A. 99*, 11998–12000.
40. Dekker, N. H., Rybenkov, V. V., Duguet, M., Crisona, J. J., Cozarelli, N. R., Bensimon, D., and Croquette, V. (2002) The mechanism of type 1A topoisomerases. *Proc. Natl. Acad. Sci. U.S.A. 99*, 12126–12131.

41. Champoux, J. J. (2001) DNA topoisomerases: structure, function and mechanism. *Annu. Rev. Biochem. 70*, 369–413.
42. Vologodskii, A. V., and Cozzarelli, N. R. (1994) Conformational and thermodynamic properties of supercoiled DNA. *Annu. Rev. Biophys. Biomol. Struct. 23*, 609–643.
43. Rangel, D. P., Fujimoto, B. S., and Schurr, J. M. (2008) Estimation of the persistence length of DNA from the torsion elastic constant and supercoiling free energy: Effect of ethylene glycol. *J. Phys. Chem. B 112*, 13359–13366.
44. Stevnsner, T., Mortensen, U. H., Westergaard, O., and Bonven, B. J. (1989) Interactions between a eukaryotic DNA topoisomerase I and a specific binding sequence. *J. Biol. Chem. 264*, 10110–10113.
45. Zechiedrich, E. L., and Osheroff, N. (1990) Eukaryotic topoisomerases recognize nucleic acid topology by DNA crossovers. *EMBO J. 9*, 4555–4562.
46. Fujimoto, B. S., and Schurr, J. M. (2002) Monte Carlo simulations of supercoiled DNAs confined to a plane. *Biophys. J. 82*, 944–962.
47. White, J. H. (1969) Self-linking and Gauss-integral in higher dimensions. *Am J. Math. 91*, 693–728.
48. Fuller, F. B. (1971) Writhing number of a space curve. *Proc. Natl. Acad. Sci. U.S.A. 68*, 815–819.
49. Camilloni, G., Di Martineo, E., Caserta, M., and Di Mauro, E. (1988) Eukaryotic DNA topoisomerase I reaction is topology dependent. *Nucleic Acids Res. 16*, 7071–7085.
50. Camilloni, G., Di Martino, E., Di Mauro, E., and Caserta, M. (1989) Regulation of the function of eukaryotic DNA topoisomerase I: Topological conditions for non-reactivity. *Proc. Natl. Acad. Sci. U.S.A. 86*, 3080–3084.
51. Caserta, M., Amadei., A., Camilloni, G., and Di Mauro, E. (1990) Regulation of the function of eukaryotic DNA topoisomerase I: Analysis of the binding step and catalytic constants of topoisomerization as a function of DNA topology. *Biochemistry 29*, 8152–8157.
52. Shuman, S., Bear, D. G., and Sekiguchi, J. (1997) Intramolecular synapsis of duplex DNA by *Vaccinia* topoisomerase. *EMBO J. 16*, 6584–6587.
53. Moreno-Herrero, F., Holtzer, L., Koster, D. A., Shuman, S., Dekker, C., and Dekker, N. H. (2005) Atomic force microscopy shows that *Vaccinia* topoisomerase Ib generates filaments on DNA in cooperative fashion. *Nucleic Acids Res. 33*, 5945–5943.
54. Yang, Z., Carey, J. F., and Champoux, J. J. (2009) Mutational analysis of the preferential binding of human topoisomerase I to supercoiled DNA. *FEBS J. 276*, 5906–5919.
55. Stevens, M. J. (2001) Simple simulations of DNA condensation. *Biophys. J. 80*, 1130–139.
56. Ou, Z., and Muthukumar, M. (2005) Langevin dynamics of semiflexible polyelectrolytes: Rod-toroid-globule structures and counterion distribution. *J. Chem. Phys. 123*, 07905–1−07905−9.
57. Borukhov, I., Bruinsma, R., Gelbart, W. M., and Liu, A. J. (2001) Elastically driven linker aggregation between two semi-flexible polyelectrolytes. *Phys. Rev. Lett. 86*, 2182–2185.
58. Crut, A., Koster, D. A., Seidel, R., Wiggins, C. H., and Dekker, N. H. (2007) Fast dynamics of supercoiled DNA revealed by single-molecule experiments. *Proc. Natl. Acad. Sci. U.S.A. 104*, 11957–11962.
59. Wang, M. C., and Uhlenbeck, G. E. (1945) On the theory of Brownian motion II. *Rev. Mod. Phys. 17*, 323–342.
60. Thumm, T., Seidl, A., and Hinz, H.-J. (1988) Energy-structure correlations of plasmid DNA in different topological forms. *Nucleic Acids Res. 16*, 11737–11757.